Published in final edited form as:
Mol Biochem Parasitol. 2011 April ; 176(2): 121–126. doi:10.1016/j.molbiopara.2010.12.012.

TgVTC2 is Involved in Polyphosphate Accumulation in *Toxoplasma gondii*

Peggy J. Rooney[a], **Lawrence Ayong**[b], **Crystal M. Tobin**[a], **Silvia N.J. Moreno**[b], and **Laura J. Knoll**[a,c]

[a]Department of Medical Microbiology and Immunology, University of Wisconsin School of Medicine and Public Health, Microbial Sciences Building Room 3345, 1550 Linden Drive, Madison, WI 53706, United States

[b]Center for Tropical and Emerging Global Diseases and Department of Cellular Biology, S350A Paul D. Coverdell Center, 500 D.W. Brooks Drive, University of Georgia, Athens, GA 30602, United States

Abstract

Polyphosphate is found in every cell, having roles in diverse processes, including differentiation and response to stress. In this study, we characterize a *Toxoplasma gondii* mutant containing an insertion within the carboxy-terminal end of a homolog of *Saccharomyces cerevisiae* Vtc2p, a component of the polyphosphate synthetic machinery. Locus *TgVTC2* encodes a 140 kDa protein containing conserved SPX, VTC and transmembrane domains. TgVTC2 localizes in punctate spots within the cytoplasm that do not co-localize with known markers. The TgVTC2 mutant showed dramatically reduced polyphosphate accumulation, a defect restored by introduction of *TgVTC2* to the mutant. Insertion within *TgVTC2* resulted in increased transcript levels for two loci, including a putative FIKK kinase. These transcript levels were restored to wild-type levels upon complementation with the *TgVTC2* locus. The *TgVTC2* locus was refractory to knockout, and may be essential. Analysis of this TgVTC2 mutant will facilitate dissection of the *T. gondii* polyphosphate synthesis pathway.

Keywords

Toxoplasma; polyphosphate; SPX; VTC; Q-PCR; FIKK kinase

Introduction, results, and discussion

Polyphosphate is comprised of chains of tens to hundreds of orthophosphate residues linked by phosphoanhydride bonds. This polymer is found in every cell in nature, and may have played a role in the primordial synthesis of nucleic acids. In prokaryotic and eukaryotic microbes, this polymer has roles in diverse cellular processes, including cation sequestration, cell envelope formation, regulation of gene expression and enzyme activities, regulation of development, stationary-phase adaptation, and mediating responses to alkaline

[c]Corresponding author, tel: +1 608 2623161; fax: +1 608 2628418; ljknoll@wisc.edu.

or osmotic stress, as well as having the potential to act as a reserve energy source [1]. In parasites, polyphoshate is concentrated within a specialized organelle, the calcium-rich acidocalcisome [2]. Changes in cellular polyphosphate levels were associated with differentiation of *Trypanosoma cruzi*, as well as exposure to osmotic and alkaline stress, suggesting a role in adaptation to environmental change [3]. Disruption of polyphosphate metabolism affects the response to phosphate starvation and osmotic stress in *T. brucei* [4], and virulence in mice in *Leishmania amazonensis* [5]. In *Toxoplasma gondii*, polyphosphate levels change in response to stress. Deletion of Ca+/H+-ATPase *TgA1* in *T. gondii* resulted in reduced polyphosphate levels and decreased virulence in mice [6], furthering the linkage of these phenotypes. Despite the importance of polyphosphate, the synthetic machinery for creation of this molecule has only recently been described in *Saccharomyces cerevisiae* [7]. Here, we characterize an insertion mutant of *T. gondii* showing reduced polyphophate levels, uncovering a component of the polyphosphate synthetic machinery in this parasite.

Insertion mutant 18C5 was identified in a signature-tagged mutagenesis screen by its reduced ability to form cysts in the brains of experimentally infected mice (data not shown) [8]. Plasmid rescue identified the disrupted locus in 18C5 as being on chromosome 11, within the coding region of gene prediction TgME49_098630, as annotated in the *T. gondii* genome database (ToxoDB v6, http://toxodb.org). This locus encodes a protein predicted to be 1308 amino acids and 141.6 kDa, containing an amino-terminal SPX domain (amino acid position 1 through 287, E-value = 3×10^{-36}) followed by a VTC domain (position 398 to 801, E-value = 6.9×10^{-16}), and a near-carboxy-terminal transmembrane region (DUF202, position 1075–1131, E-value = 2.5×10^{-11}), as identified by Pfam v24.0 (http://pfam.sanger.ac.uk). The SPX domain (PF03105), named for family members SYG1, Pho81 and XPR1, is found in the amino terminus of proteins involved in the regulation of phosphate transport. Many proteins bearing SPX domains are suggested to be involved in G-protein associated signal transduction [9]. The VTC domain (PF09359) is found in yeast vacuolar transporter chaperones Vtc2p, Vtc3p and Vtc4p [10,11]. DUF202 (PF02656) stands for domain of unknown function, as this region has not been characterized. However, this domain contains predicted transmembrane regions, and many family members are putative membrane proteins. The TgME49_098630 disruptant contains a plasmid insertion in the extreme 3' end of the open reading frame, downstream of the predicted transmembrane domain, and only 13 amino acids from the C-terminus of the predicted protein (Fig. 1A).

The identical arrangement of amino-terminal SPX, central VTC and carboxy-terminal DUF202 domains is also found in the Vtc2p, Vtc3p, and Vtc4p proteins of *S. cerevisiae* and their homologs. In yeast, the VTC proteins form hetero-oligomeric complexes that synthesize and transfer polyphosphate to vacuoles, as well as impacting membrane trafficking and vacuole fusion [7,10–13]. Of these proteins, Vtc4p was recently identified as the polyphosphate synthase in *S. cerevisiae*, although mutants in each of the VTC proteins resulted in reduced accumulation of polyphosphate [7,12]. Vtc2p and Vtc3p show strong similarity to Vtc4p, but lack critical active site residues and appear to be accessory subunits in the VTC complex. These proteins form functional oligomers of either Vtc2p or Vtc3p, together with Vtc4p and Vtc1p [7]. Three SPX domain-containing proteins are found in the *T. gondii* genome, annotated as TgME49_098630, TgME49_048550, and TgME49_113870 (ToxoDB). Also, basic local alignment search tool (BLAST) analysis of ToxoDB using the TgME49_098630 protein identified a homolog and additional candidate VTC, TgME49_099080. The TgME49_048550 and TgME49_113870 contain SPX, but neither VTC nor DUF202 domains. TgME49_099080 shares the VTC and DUF202 domains with TgME49_098630, but lacks an SPX domain. Within these VTC domains, only TgME49_099080 contains a lysine (K769) aligning with the catalytic lysine identified in Vtc4p of *S. cerevisiae*, critical for polyphosphate synthesis [7]. The locus disrupted in 18C5

bears homology to both Vtc2p and Vtc3p, with a slightly higher ClustalW alignment score with Vtc2p, which, like Vtc3p, affects vacuolar polyphosphate accumulation and membrane trafficking in *S. cerevisiae*. As such, the locus identified in this study will be called *TgVTC2*.

To confirm that this locus was disrupted in 18C5, a 1.8 kb fragment matching a polyadenylated expressed sequence tag (EST TgDT.336204.tmp; ToxoDB) predicted to contain the final exon and 3' untranslated region (UTR), was used to probe total RNA from both the insertion mutant and Pru. The *TgVTC2* transcript was detected in Pru as approximately 6 kb size, but was found to be larger in the insertion mutant, indicating transcription into the plasmid sequences used for insertional mutagenesis (Fig. 1B). It is possible that TgVTC2 is translated in 18C5, although with an alternate carboxy-terminal sequence. The wild-type protein from Pru terminates with a helix downstream of the insertion site AAAEGARVTAGAK*), while the insertion mutant protein, if translated, would contain a 24 amino acid replacement predicted to be a hydrophilic stretch AASTKPPSRQVSVMLCQCYNQLTNSD*). Replacement of the native 3' UTR may also impact the translational efficiency of TgVTC2 in the mutant.

The nucleotide sequence of the wild-type *TgVTC2* transcript was determined. The 3927 nucleotide *TgVTC2* coding region was amplified from Pru cDNA, and matched the sequence and intron-exon structure predicted for TgME49_098630 (ToxoDB). Transcript ends were defined by rapid amplification of cDNA ends (RACE), from which the 5' end was found to be 823 bases upstream of the translational start site, 47 bases farther upstream than that predicted by ToxoDB for strain ME49. We identified a predicted 367 bp intron within the 5' UTR, which was found both spliced and unspliced in mature transcripts, as determined by analysis of cDNA amplification products. This intron sequence was used to probe total RNA from Pru, and hybridized to a band of equivalent size to that seen with the 1.8 kb 3' probe (data not shown). The 3' RACE demonstrated multiple transcript termini 1121 to 1259 nucleotides downstream of the translational stop codon, whereas EST TgDT.336204.tmp is 1388 nucleotides downstream of the stop site.

To assess the role of TgVTC2 in both formation of cysts in vivo, and polyphosphate accumulation in vitro, the intact *TgVTC2* cDNA was assembled. Constructs contained the coding region along with 1538 bp of downstream sequence, and 1817 bp of upstream sequence predicted to contain the *TgVTC2* promoter region, with (pTPR2) or without (pTPR1) the intron in the 5' UTR (Supplementary Material 1; Table S1; Fig. S1). To facilitate detection of TgVTC2, plasmid pTPR2HA included an additional amino-terminal influenza hemagglutinin (HA) tag upstream of the initiator methionine. The tag followed a synthetic initiator methionine and alanine linker, added to create an optimal translational initiation context [14]. Plasmids were electroporated into *T. gondii* 18C5. Expression of the intact *TgVTC2* transcript was confirmed by northern hybridization (data not shown). Expression of HA-tagged TgVTC2 was confirmed by western immunoblot, which indicated a protein doublet migrating at about 140 kDa (Fig. 1C). To determine if TgVTC2 affects in vivo cyst formation, 18C5, Pru and 18C5 transformants were used to infect CBA/J mice, along with parental strain C5, the signature-tagged strain from which 18C5 was derived [8]. Four weeks post-infection, cyst formation in brains was quantified by immunofluorescence microscopy as previously described [8]. The C5 parental strain showed a severe in vivo cyst formation defect in comparison to Pru, likely due to insertion of the first, tag-containing plasmid. This prevented assessment of the contribution of the second plasmid insertion, within *TgVTC2*, to establishment of chronic infection. Despite numerous attempts, we were unable to create a knockout of the *TgVTC2* locus (data not shown), leading to an inability to determine its impact on virulence in vivo. This result could indicate that *TgVTC2* is an essential gene. Alternatively, this could be due to its subtelomeric location on chromosome 11 of the *T. gondii* genome (ToxoDB). The insertion mutant was obtained using restriction

endonuclease-mediated integration, which may have enhanced recombination of transforming DNA at this site.

As accumulation of polyphosphate was affected in a *VTC2* mutant of *S. cerevisiae*, polyphosphate levels were assessed in the 18C5 mutant. The steady-state levels of long- (>25 units) and short-chain polyphosphate were determined for C5, 18C5, and full-length *TgVTC2* transcript-expressing transformants 18C5/pTPR1 and 18C5/pTPR2HA. The 18C5 mutant had marked decreases in long- and short-chain polyphosphates compared to C5, which are partially restored in the 18C5 transformants by addition of an intact copy of the *TgVTC2* locus (Fig. 2A; Fig. S2). An 18C5/pTPR2 transformant, expressing untagged TgVTC2, showed similar partial restoration of long-chain polyphosphate accumulation in comparison to 18C5 (data not shown). These data demonstrate that despite the absence of the active site residues such as those found in the polyphosphate synthetic enzyme Vtc4p of *S. cerevisiae*, TgVTC2 impacts the levels of long-chain polyphosphates, as does Vtc2p, its enzymatically inactive homolog in yeast. Additionally, the intron found in the 5'UTR of *TgVTC2* was not required for phenotypic complementation. Polyphosphate has been implicated in mediating responses to stress, including conditions stimulating differentiation. Deletion of *vtc4* in the pathogenic fungus *Ustilago maydis* impacts both virulence and morphogenesis to the invasive filamentous form [16]. In *T. cruzi*, a rapid increase in polyphosphate was associated with trypomastigote to amastigote differentiation [3]. To determine if disruption of *TgVTC2* impacts differentiation, we subjected strains 18C5, C5 and Pru to conditions of elevated pH (8.1), reduced serum content (1%), and ambient CO_2 for three days, commonly used to stimulate in vitro bradyzoite development at 37°C. Resulting bradyzoite conversion within human foreskin fibroblast monolayers was assessed by reacting formalin-fixed cells with fluorescein isothiocyanate (FITC)-conjugated *Dolichos biflorus* agglutinin, followed by analysis by fluorescence microscopy. All three strains showed similar reactivity, indicating that the *TgVTC2* disruptant is capable of undergoing in vitro bradyzoite conversion, despite the reduction in stored long-chain polyphosphates (data not shown).

Two polyphosphate synthetic complexes have been identified in yeast, comprised of either Vtc1/3/4p or Vtc1/2/4p, with the former appearing in or on vacuoles, while the latter was found to be partially on vacuoles, but also perinuclear and in patches along the plasma membrane [7]. To determine the localization of TgVTC2, an 18C5/pTPR2HA transformant expressing the tagged protein from the predicted *TgVTC2* promoter was examined by immunofluorescence deconvolution microscopy. TgVTC2 was expressed in punctate spots within the cytoplasm of both intracellular and extracellular tachyzoites, which did not colocalize with markers of known subcellular compartments of *T. gondii*, including micronemes, rhoptries, dense granules, or the recently identified plant-like vacuole (Fig. 1D). Interestingly, it also did not colocalize with the TgVP1 marker of acidocalcisomes, despite this organelle having been noted as a polyphosphate depot [2]. Though addition of the HA tag and ectopic integration of the pTPR2HA vector may influence localization, tagged TgVTC2 complemented the polyphosphate accumulation defect of 18C5, indicating the protein is functional.

A gene expression microarray-based approach was initiated to elucidate downstream effects of the *TgVTC2* disruption in the 18C5 mutant. Custom tiled arrays containing *T. gondii* genomic oligonucleotides were hybridized with cDNA probes derived from tachyzoite-stage parasites of strains 18C5, C5 and Pru (Roche NimbleGen, Madison, WI). Of the hybridization results, only five loci were identified as distinct in their expression in 18C5 as compared to both C5 and Pru, with a false discovery rate cutoff of 1×10^{-7}. These loci included a predicted FIKK kinase (TgME49_089050), TgPLP1 (TgME49_004130), and three genes whose predicted products have no known homologs (TgME49_112140,

TgME49_070820, and TgME49_005280). Interestingly, TgPLP1 and TgME49_005280 were downregulated in 18C5, while the predicted FIKK kinase, TgME49_070820, and TgME49_112140 were shown to be upregulated in 18C5 relative to strains C5 and Pru (data not shown). To confirm the validity of these microarray data, quantitative real-time PCR (Q-PCR) was performed on these five loci, as well as constitutive gene *GRA2* (TgME49_027620) and housekeeping gene *TUB1* (TgME49_116400), using cDNA from strains 18C5, C5, and complementation clones 18C5/pTPR2#2–19 and 18C5/pTPR2HA. Transcription of the TgME49_070820 locus was undetectable over background by Q-PCR, which is in keeping with previous data indicating weak expression (Anderson and Boothroyd, unpublished results available at ToxoDB). Although a trend towards down-regulation of *TgPLP1* and TgME49_005280 in 18C5 relative to C5 was noted in each replicate, it was not statistically significant, though these transcripts were increased in the complemented strains over levels seen in the mutant (Fig. S3). No significant differences were noted in transcription of *GRA2* between the tested strains (data not shown). In contrast, transcriptional upregulation of both the FIKK kinase and TgME49_112140 locus in 18C5 was confirmed by Q-PCR ($p < 0.02$). Expression of FIKK kinase was increased by approximately 6-fold, while TgME49_112140 showed a more modest 2.3-fold increase in expression in 18C5 compared to C5 (Fig. 2B). Complementation of the intact *TgVTC2* locus reduced transcription of these loci to the levels found in strain C5.

The protein product of TgME49_112140 is predicted to be 50 kDa, and is conserved between *T. gondii* and *Neospora caninum*. Although similar proteins are found in *Plasmodium* species, this predicted protein lacks conserved domains, or orthologs outside of phylum Apicomplexa, as determined by the BLASTp algorithm (http://blast.ncbi.nlm.nih.gov/Blast.cgi). The predicted *T. gondii* FIKK kinase is a member of a recently described family of proteins sharing a non-canonical C-terminal kinase domain lacking a complete glycine triad, which is involved in positioning ATP within the catalytic cleft in most, but not all other eukaryotic protein kinases [17]. Despite this domain architecture, these proteins possess kinase activity [18]. FIKK kinases are found only within Apicomplexa, with most species expressing a single ortholog, while the *P. falciparum* genome was found to contain 20 paralogs. The first of these kinases identified was trophozoite protein R45 of *P. falciparum* (PFD1175w), a vaccine candidate that is exported to the erythrocyte cell membrane [19]. Like TgME49_112140, the FIKK kinases are highly homologous amongst *T. gondii* species (E-value=0, 97–99% identity) and similar to those found in *Cryptosporidium* and *Plasmodium* species (E-value range = 6×10^{-71} to 3×10^{-32}, determined by BLASTp).

In this study, we characterized *TgVTC2*, a locus in *T. gondii* that expresses a product bearing homology to Vtc2p of *S. cerevisiae*. Plasmid insertion within this locus reduced the ability of the parasite to store wild-type levels of long chain polyphosphate. Similarly, downregulation of Vtc1p-homolog TbVTC1 in *T. brucei* led to reduced polyphosphate production, as well as altering the morphology and function of the acidocalcisome [20]. Though there is a clear phenotypic change in the TgVTC2 disruptant, it is unclear if TgVTC2 is absent or is expressed with an alternate carboxy-terminus in 18C5. The sequences found downstream of the DUF202 transmembrane domain may be important for association with other components of the VTC complex in *T. gondii*, and/or may play a role in signaling events. We speculate that the VTC complex of *T. gondii* may assemble to a structure similar to that seen in *S. cerevisiae*. In this case, TgVTC2 may couple with TgME49_099080, the predicted synthetic component of VTC. In yeast, the transmembrane domain of Vtc4p is predicted to be supplemented functionally by that of Vtc1p, which contains only the DUF202 domain. When coupled with either Vtc2p or 3p, this trimer could then act as a functional dimer. In *T. gondii*, Vtc4p homolog TgME49_099080 is instead lacking the SPX domain, but contains VTC and DUF202 domains. It is possible that either

TgME49_048550 or TgME49_113870 could donate an SPX domain to TgME49_099080 to form a trimer with TgVTC2. VTC complexes are predicted to be membrane associated, and expectedly, TgVTC2 associates with membrane fractions in mass spectrometry studies (J.M. Wastling, University of Liverpool, and Albert Einstein Biodefense Proteomics Research Center; unpublished results available at ToxoDB). Interestingly, these studies did not show TgME49_099080 in membrane fractions. Association with TgVTC2 may offer correct localization to the enzymatic portion of the complex.

We were surprised to find two loci upregulated in the TgVTC2 disruptant. The function and phosphorylation targets of FIKK kinases are unknown. Upregulation of this kinase in *T. gondii* in response to a loss of TgVTC2 activity is the first demonstration of FIKK kinase expression correlating to a biological function, suggesting the intersection of FIKK kinase with the polyphosphate signaling cascade.

Supplementary Material

Refer to Web version on PubMed Central for supplementary material.

Abbreviations

VTC	vacuolar transporter chaperone
DUF	domain of unknown function
BLAST	basic local alignment search tool
E-value	expect value
ToxoDB	*Toxoplasma* genome database
EST	expressed sequence tag
Pru	Prugniaud
RACE	rapid amplification of cDNA ends
HA	hemagglutinin
FITC	fluorescein isothiocyanate
DAPI	4’-6-diamidino-2-phenylindole
Q-PCR	quantitative real-time PCR
GRA	dense granule protein
TUB1	alpha tubulin
TgPLP1	perforin-like protein 1
TgCPL	cathepsin L
TgVP1	vacuolar-type H(+)-pyrophosphatase 1
MIC2	microneme protein 2
TgA1	acidocalcisome Ca^{2+}-ATPase 1
HFF	human foreskin fibroblast
FBS	fetal bovine serum
rPPX1	recombinant exopolyphosphatase
Pi	inorganic phosphate

Acknowledgments

We are grateful to Kami Kim (Albert Einstein College of Medicine, Bronx, NY) for use of tiled *T. gondii* microarrays, and Manuel Garber and John Rinn (Broad Institute of MIT and Harvard, Cambridge, MA, United States) for providing use of a pre-release version of a java-based tiled gene expression microarray analysis package. Rabbit antisera was provided by L.D. Sibley, Washington University School of Medicine, St. Louis, MO (MIC2), I. Coppens, Johns Hopkins Malaria Research Institute, Baltimore, MD (GRA2 and GRA7), and V. Carruthers, University of Michigan Medical School, Ann Arbor, MI (TgCPL). We thank Alyssa Smith and Kyle Boldon for technical assistance. This work was supported by National Research Service Award number F32AI065023 from the National Institute of Allergy and Infectious Diseases (NIAID) to PJR, NIAID 5R03AI077345 and American Cancer Society RSG-07-202-01-MBC to LJK, and NIAID 5R21AI079625 to SNJM. The content is solely the responsibility of the authors and does not necessarily represent the official views of the NIAID or the National Institutes of Health.

References

1. Kulaev I, Kulakovskaya T. Polyphosphate and phosphate pump. Ann Rev Microbiol 2000;54:709–734. [PubMed: 11018142]
2. Rodrigues CO, Ruiz FA, Rohloff P, Scott DA, Moreno SNJ. Characterization of isolated acidocalcisomes from *Toxoplasma gondii* tachyzoites reveals a novel pool of hydrolyzable polyphosphate. J Biol Chem 2002;277:48650–48656. [PubMed: 12379647]
3. Ruiz FA, Rodrigues CO, Docampo R. Rapid changes in polyphosphate content within acidocalcisomes in response to cell growth, differentiation, and environmental stress in *Trypanosoma cruzi*. J Biol Chem 2001;276:26114–26121. [PubMed: 11371561]
4. Lemercier G, Espiau B, Ruiz FA, Vieira M, Luo S, Baltz T, et al. A pyrophosphatase regulating polyphosphate metabolism in acidocalcisomes is essential for *Trypanosoma brucei* virulence in mice. J Biol Chem 2004;279:3420–3425. [PubMed: 14615483]
5. Espiau B, Lemercier G, Ambit A, Bringaud F, Merlin G, Baltz T, et al. A soluble pyrophosphatase, a key enzyme for polyphosphate metabolism in *Leishmania*. J Biol Chem 2006;281:1516–1523. [PubMed: 16291745]
6. Luo S, Ruiz FA, Moreno SNJ. The acidocalisome Ca^{2+}-ATPase (*TgA1*) of *Toxoplasma gondii* is required for polyphosphate storage, intracellular calcium homeostasis and virulence. Mol Microbiol 2005;55:1034–1045. [PubMed: 15686552]
7. Hothorn M, Neumann H, Lenherr ED, Wehner M, Rybin V, Hassa PO, et al. Catalytic core of a membrane-associated eukaryotic polyphosphate polymer. Science 2009;324:513–516. [PubMed: 19390046]
8. Frankel MB, Mordue DG, Knoll LJ. Discovery of parasite virulence genes reveals a unique regulator of chromosome condensation 1 ortholog critical for efficient nuclear trafficking. Proc Natl Acad Sci USA 2007;104:10181–10186. [PubMed: 17535896]
9. Spain BH, Koo D, Ramakrishnan M, Dzudzor B, Colicelli J. Truncated forms a novel yeast protein suppress the lethality of a G protein alpha subunit deficiency by interacting with the beta subunit. J Biol Chem 1995;270:25435–25444. [PubMed: 7592711]
10. Cohen A, Perzov N, Nelson H, Nelson N. A novel family of yeast chaperons involved in the distribution of V-ATPase and other membrane proteins. J Biol Chem 1999;274:26885–26893. [PubMed: 10480897]
11. Müller O, Bayer MJ, Peters C, Anderson JS, Mann M, Mayer A. The Vtc proteins in vacuole fusion: coupling NSF activity to V(0) trans-complex formation. EMBO J 2002;21:259–269. [PubMed: 11823419]
12. Ogawa N, DeRisi J, Brown PO. New components of a system for phosphate accumulation and polyphosphate metabolism in *Saccharomyces cerevisiae* revealed by genomic expression analysis. Mol Bio Cell 2000;11:4309–4321. [PubMed: 11102525]
13. Müller O, Neumann H, Bayer MJ, Mayer A. Role of Vtc proteins in V-ATPase stability and membrane trafficking. J Cell Sci 2002;116:1107–1115.
14. Seeber F. Consensus sequence of translational initiation sites from *Toxoplasma gondii* genes. Parasitol Res 1997;83:309–311. [PubMed: 9089733]

15. Baykov AA, Evtushenko OA, Avaeva SM. A malachite green procedure for orthophosphate determination and its use in alkaline phosphatase-based immunoassay. Anal Biochem 1988;171:266–270. [PubMed: 3044186]

16. Boyce KJ, Kretschmer M, Kronstad JW. The *vtc4* gene influences polyphosphate storage, morphogenesis, and virulence in the maize pathogen *Ustilago maydis*. Euk Cell 2006;5:1399–1409.

17. Ward P, Equinet L, Packer J, Doerig C. Protein kinases of the human malaria parasite *Plasmodium falciparum*: the kinome of a divergent eukaryote. BMC Genomics 2004;5:79. [PubMed: 15479470]

18. Nunes MC, Goldring JP, Doerig C, Scherf A. A novel protein kinase family in *Plasmodium falciparum* is differentially transcribed and secreted to various cellular compartments of the host cell. Mol Microbiol 2007;63:391–403. [PubMed: 17181785]

19. Schneider AG, Mercereau-Puijalon O. A new *Apicomplexa*-specific protein kinase family: multiple members in *Plasmodium falciparum*, all with an export signature. BMC Genomics 2005;6:30. [PubMed: 15752424]

20. Fang J, Rohloff P, Miranda K, Docampo R. Ablation of a small transmembrane protein of *Trypanosoma brucei* (TbVTC1) involved in the synthesis of polyphosphate alters acidocalcisome biogenesis and function, and leads to a cytokinesis defect. Biochem J 2001;407:161–170. [PubMed: 17635107]

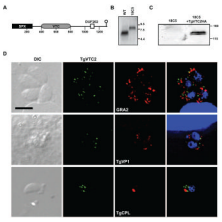

Figure 1.

A. Domain map of TgME49_098630 (TgVTC2). Shown are the relative positions of SPX, VTC and DUF202 domains. The site of insertion in strain 18C5 is indicated as a lollipop. Amino acid distance markers are shown under the cartoon.

B. Strain 18C5 is disrupted in predicted gene TgME49_098630. Parasites were grown in human foreskin fibroblasts (HFF) cultivated in Dulbecco's modified eagle medium (DMEM) containing 10% fetal bovine serum (FBS). Total RNA was derived from approximately 1×10^7 intracellular tachyzoites of strains Pru (WT) and 18C5 by passage through a 27-gauge needle, centrifugation at 425×g for 10 min, and processing of the pellet with ULTRASPEC (BiotecX). RNA was separated by formaldehyde agarose gel electrophoresis, transferred to nytran, and probed with a radiolabeled (Random Primed DNA Labeling Kit, Roche) cloned DNA fragment amplified using primer 5'-CGATTCTCGTAGTCACACTGATGC and the 3' RACE Inner Primer (FirstChoice RLM-RACE, Ambion Inc.). RNA size standards are indicated to the right in kilobases.

C. Amino-terminal HA-tagged TgVTC2 migrates as a dimer around 140 kDa. Of strains 18C5 and 18C5/pTPR2HA (18C5+TgVTC2HA), 2×10^7 extracellular tachyzoites lysed from HFFs were harvested by centrifugation at 425×g for 10 min, and pellets were suspended in denaturing protein sample buffer and boiled for 10 minutes. Samples were separated on 8% polyacrylamide gels, transferred to nitrocellulose, reacted with monoclonal anti-HA antibody (clone 16B12, #MMS-101R, Covance, Emoryville, CA), and detected with ECL Plus western blotting detection system (GE). Molecular mass standards are shown at the right in kDa.

D. TgVTC2 localizes within the cytoplasm. Confluent coverslips of HFFs were infected with tachyzoites of strain 18C5/pTPR2HA. Twenty-eight hours post-infection, monolayers were fixed with PBS/3% methanol-free fomaldehyde, blocked with PBS/3% BSA/0.2% triton X-100. TgVTC2 was detected with mouse monoclonal anti-HA (Covance) and AlexaFluor488. Subcellular compartments were defined with the following rabbit antisera: anti-MIC2 (micronemes), anti-GRA2 or anti-GRA7 (dense granules), and anti-TgVP1 (acidocalcisomes). Naturally egressed tachyzoites were fixed to coverslips and similarly reacted with rabbit anti-TgCPL (plant-like vacuole). These markers were detected with AlexaFluor633. Coverslips were mounted with VectaShield with DAPI (Vector Laboratories, Inc). Fluorescent images were captured using a Zeiss Axioplan 2 microscope and OpenLab 5.0.1 imaging software (PerkinElmer), and deconvolved using Volocity 4 (PerkinElmer). Shown are DIC images (left), 488 nm (TgVTC2) and 633 nm (GRA2, TgVP1 or TgCPL) channels and a composite image (right) including the DNA detection reagent DAPI. All images are identical in scale, and a 5 μm bar is indicated.

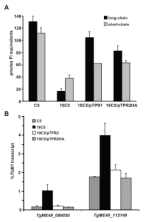

Figure 2.

A. The *TgVTC2* disruptant strain shows reduced polyphosphate content in tachyzoites. Parasites for polyphosphate extraction were grown in h-Tert HFFs in DMEM containing 1% FBS. Extracellular tachyzoites were collected by centrifugation and washed twice with 116 mM NaCl, 5.4 mM KCl, 0.8 mM $MgSO_4$, 50 mM HEPES, pH 7.2, 5.5 mM glucose. Long chain polyphosphate (average size ≥ polyP25 standards, Sigma) was extracted by TRI Reagent RNA isolation (Sigma). Short chain polyphosphate was extracted as previously described [2,3]. Polyphosphate content was determined by measuring inorganic phosphate (Pi) release upon incubation with recombinant *S. cerevisiae* exopolyphosphatase (rPPX1) purified from *E. coli* strain CA38 pTrcPPX1 [3] using malachite green as previously described [15]. Results are shown for strains C5, 18C5, and two 18C5 transformants. 18C5/pTPR1 contains the *TgVTC2* cDNA lacking the intron in the 5' UTR, while 18C5/pTPR2HA contains the intron, and an amino-terminal HA tag. Shown are average values per million tachyzoites from two (long-chain polyphosphate) or three (short-chain polyphosphate) independent samples, and standard deviations. The standard deviation for short-chain polyphosphate values from 18C5/pTPR1 is 0.01 pmol P_i equivalents. Student's t-tests indicate long- and short-chain polyphosphate levels of the complements are significantly higher than those of the mutants ($p<0.002$).

B. TgME49_112140 and TgME49_089050 (FIKK kinase) transcripts are upregulated in the *TgVTC2* mutant. Total RNA from strains C5 (gray bars), 18C5 (black bars), 18C5/pTPR2#2–19 (white bars), and 18C5/pTPR2HA (hatched bars) was isolated from intracellular tachyzoites in HFFs 48h post-infection as described. RNA was treated with amplification grade DNase I (Invitrogen), and 2μg was subjected to random hexamer-based cDNA synthesis by Superscript III first-strand synthesis system (Invitrogen). Transcript levels were measured with primer sets 5'-AGAAACAGACAAGACCCCATTAC and 5'-GAACCTTGTTGTCATCTGGAGAAG (TgME49_089050), 5'-CGTGCTGCCTCTCTGTCTCAAATG and 5'-TGCAAACCTGGAGGCTCCGAGAAG (TgME49_112140), 5'-GACGTGCCTTTCAGCGGTAAAC and 5'-CCGGTTCTTCTGGCTCTTGTTG (TgME49_027620, *GRA2*), and 5'-GACGACGCCTTCAACACCTTCTTT and 5'-AGTTGTTCGCAGCATCCTCTTTCC (TgME49_116400, α-tubulin, *TgTUB1*) by quantitative PCR (Q-PCR). Reactions were performed on an iCycler in a 25 μl volume, using iQTM SYBR® Green Supermix, and results were analyzed with iQTM software v. 3.1 (Bio-Rad). Water and DNase-treated RNA without reverse transcription did not yield detectable threshold cycles (Ct). Melt curve analyses were performed on each sample to ensure product specificity. Primer set efficiencies (E) were determined by Q-PCR reactions using 10-fold serial dilutions of template, plotting Ct values against log template to determine the slope of the line (m), and represents the average of three experiments. Results for each sample were adjusted for primer efficiency differences using Pfaffl's modification of the delta Ct method, and test transcript levels were normalized to *TgTUB1* levels using the following formula $(E_{TgTUB1}{}^{Ct})/(E_{\text{test gene}}{}^{Ct})$, where $E=10^{(1/m)}$. Shown is the average and standard deviation, derived from three independent RNA samples per strain, and *p*-values were generated by the student's *t*-test.